Geometry-independent neutral desorption device for the sensitive EESI-MS detection of explosives on various surfaces†

Haiwei Gu,[a] Shuiping Yang,[a] Jianqiang Li,[a] Bin Hu,[a] Huanwen Chen,*[a] Lili Zhang[b] and Qiang Fei[b]

Received 14th October 2009, Accepted 1st February 2010
First published as an Advance Article on the web 26th February 2010
DOI: 10.1039/b921579d

A novel geometry-independent neutral desorption (GIND) device was successfully developed, which made neutral desorption (ND) sampling easier and more robust on virtually all types of surfaces. The GIND device features a small air-tight enclosure with fixed space between the ND gas emitter, the sample surface, and the sample collector. Besides easy fabrication and convenient use, this configuration facilitates efficient neutral sample transfer and results in high sensitivity by preventing material loss during the ND process. The effects of various operating parameters of the GIND device such as desorption gas composition, surface wetness, gas flow rate, distance between the surface and the gas emitter, internal diameter of the sample outlet, and GIND device material were experimentally investigated. By using the GIND device, trace amounts of typical explosives such as TNT, RDX, HMX, TATP, *etc.*, were successfully sampled from many different kinds of surfaces, including human skin, glove, glass, envelope, plastic, leather, glass, and clothes. GIND-sampled explosives were detected by multiple-stage extractive electrospray ionization mass spectrometry (EESI-MS). Ion/molecule reactions of explosives such as RDX and TATP were implemented in the EESI source for the rapid detection with enhanced sensitivity and specificity. The typical time for a single sample analysis was a few seconds. Successful transportation of the neutral analytes over a distance longer than 10 m was demonstrated, without either significant signal loss or serious delay of signal response. The limit of detection for these explosives in the study was in the range of *ca.* 59–842 fg ($S/N = 3$, $n = 8$) on various surfaces. Acceptable relative standard deviation (RSD) values (*ca.* 4.6–10.2%, $n = 8$) were obtained for all the surfaces tested, showing the successful sampling of trace non-volatile explosive compounds (sub-picogram) by the GIND device for the EESI mass spectrometric analysis.

1. Introduction

Explosive detection is of sustainable interest because many explosives have genetic toxicity[1,2] and worldwide explosive abuse brings a serious threat to human society. As explosives are non-volatile at room temperature, they are of high affinities to the surfaces of objects exposed to them. Explosives are relatively soluble in fat rather than in water, which makes the oily surface (*e.g.*, human skin) a good substrate to accumulate explosives. In the real word, explosives, usually trace amounts, coexist with numerous compounds which compose a complex matrix challenging the detection of the explosive.[3,4] A useful analytical tool for explosives detection requires high sensitivity, high throughput, and high specificity.[5–7] Remote analysis where system operators and expensive instruments are operable remotely is also desirable, especially for the cases with extreme environmental conditions (*e.g.*, low temperature, high risk, biohazards) to which only a cheap sensor or a sampling device should be exposed.

Many techniques such as ion mobility spectrometry,[4,8,9] optical sensors,[3,10–12] electrochemical sensors,[13–16] chromatography,[10,17–19] and mass spectrometry[5,6,20–23] have been used for explosives detection. Mass spectrometry provides high sensitivity and high specificity,[5,6,24–26] thus it is the most suitable method for explosives detection. Generally, an actual sample undergoes a carefully designed procedure to clean up the matrices before sample analysis using mass spectrometry.[23,27–31] Tedious extraction, pre-separation, and pre-concentration are normally required to prepare an appropriate sample for mass spectrometric analysis.[23,27–31] This results in low efficiency and makes high-throughput explosives detection impossible. A breakthrough towards the fast analysis of complex samples was made by Cooks *et al.* using desorption electrospray ionization (DESI)[25,32,33] mass spectrometry. Following DESI, many techniques including direct analysis in real time (DART),[34,35] surface desorption atmospheric pressure chemical ionization (DAPCI),[36–39] extractive electrospray ionization (EESI),[40–42] low temperature plasma (LTP),[43,44] electrospray assisted laser desorption/ionization (ELDI),[45–47] easy ambient sonic ionization (EASI),[48–50] and dielectric barrier discharge ionization (DBDI)[21] for ambient sample analysis were reported. A major advantage of ambient mass spectrometry is that the analysis speed is significantly improved because of the minimal sample pre-treatment required. Similar to DESI, many ambient mass spectrometry techniques were initially used to directly detect analytes on solid surfaces,

[a]*Department of Applied Chemistry, East China Institute of Technology, Fuzhou, Jiangxi Province 344000, P. R. China. E-mail: chw8868@gmail.com; Fax: +86-794-8258-320*
[b]*College of Chemistry, Jilin University, Changchun, Jilin Province 130023, P. R. China*
† This paper is part of an *Analyst* themed issue on Ambient Mass Spectrometry, with guest editors Xinrong Zhang and Zheng Ouyang.

which were usually placed close to the ionization sources. Efforts have been made to extend DESI and DART for the analysis of liquid/gaseous samples, which are generally embedded in solid substrates (*e.g.*, paper) before ionization. For example, urine samples deposited on paper surfaces were successfully ionized by DESI.[51–55] In addition, liquid samples including biofluids and aerosol mixtures, and gaseous samples can be conveniently analyzed in real time using extractive electrospray ionization (EESI)[40–42] mass spectrometry without any sample pre-treatment. The unique design of EESI allows the matrices of samples to be dispersed in a relatively large spatial section formed between the neutral sample introduction channel, the primary reagent ion generation channel, and the ion inlet of the MS instrument. Thus, EESI tolerates extremely complex matrices. Heterogeneous liquid mixtures such as milk can be continuously analyzed without sensitivity loss.[56] Another merit of EESI is that samples (*e.g.*, living objects) are isolated from the direct bombardment by charged particles or energetic metastable atoms, which makes EESI attractive for monitoring biological samples[41,57–60] without either chemical contamination or sample preparation.

Using a gas beam for neutral desorption (ND), explosives on virtually any type of surfaces can be gently sampled. Coupling ND sampling to EESI separates the sampling process from the ionization process in both space and time, which results in robust ionization of complex samples with further reduced matrix effect.[41,57–60] As demonstrated in previous studies,[57,58] ND can be implemented in open air. However, the optimization of ND configuration takes about 2–30 min, largely depending on the operator's experience,[58] because the geometry-dependent setup requires careful optimization of all the parameters (*e.g.*, angles, distance) of the ND device.[58] Although a V-shaped sample collector increases the sample collection efficiency, material loss is unavoidable in the open air ND process because neutral analytes spread along the desorption gas. Motivated by highly sensitive detection and easy operation, a geometry-independent ND (GIND) device was designed for the first time and used to sample trace amounts of non-volatile analytes such as explosives for rapid extractive electrospray ionization. As demonstrated here, explosives desorbed from skin surface can be efficiently transferred over a distance longer than 10 m for detection by EESI-MS. Compared with an open-air configuration, the GIND device improves the signal of explosives by 2–3 orders of magnitude. The idea to develop a geometry-independent ND device also gives useful hints for other desorption/ionization techniques, which may be further coupled to geometry-independent devices for easier use and better performance.

2. Experimental

2.1 Reagents and materials

A series of standard explosive solutions was prepared by diluting commercially available explosive samples (1000 ppm) using methanol/water (1:1) solution, resulting in standard explosive solutions of *ca.* 1.0–100 ppt. 10 μL of each explosive solution were placed on the sample surfaces (*e.g.*, human skin, textile, *etc.*) using a micropipette, so the final amount of explosives ranged between a femtogram and several picograms. The sample spots formed in these experiments were approximately 100 mm^2, and the spot area being sampled was about 10 mm^2.

Healthy volunteers gave their consent for their skin to be *in vivo* sampled. The explosives deposited on the skin surfaces were properly washed away immediately after sampling. A commercial cotton coat worn by a volunteer was directly sampled for explosives detection. Materials such as gloves, glasses, stainless steel, *etc.* were bought from local stores for direct use without further pre-treatment. Chemicals such as RDX, TATP, HMX, and HMTD were bought from Accu Standard®, Inc. (CT, USA); TNB and NG (nitroglycerin) were bought from Dr Ehrenstorfer GmbH (Augsburg, Germany); TNT was bought from Chem Service®, Inc. (PA, USA). All chemical reagents such as acetic acid, methanol, and ammonia water solution were bought from Sinopharm Chemcial Reagent Co. Ltd (Shanghai, China) with the highest purity available and used directly without any further treatment. Deionized water was provided by the chemistry facilities of ECIT.

2.2 Geometry-independent ND device

Evolved from a typical ND device with a desorption gas emitter and a V-shaped sample collecting tube,[57,58,60] a novel GIND device was constructed by extending the V-shaped sample collector to surround the desorption gas emitter. When the novel GIND device is placed on a sample surface, an air-tight enclosure is formed between the sample surface and the sample collecting tube (schematically shown in Fig. 1), which allows the desorbed analytes to be transported to the EESI source through the sample transfer line over a long distance with minimal material loss. Theoretically, the gas emitter can be installed by forming any angle referring to the sample surface; however, to ease the fabrication, it was placed perpendicular to the sample surface. A neutral desorption gas (*e.g.*, nitrogen) beam supplied by a gas tank came out of an orifice (ID 0.1 mm; OD 1 mm) through a tube (stainless steel, ID 5.36 mm; length 5 cm), which was used as the stainless steel gas emitter. Neutral gas molecules ejected from the gas emitter impact the sample surface rapidly to facilitate neutral desorption. A layer of elastic inert rubber (thickness 2 mm) was installed along the bottom of the sample collector tube, enabling an air-tight fit of the sample collector (stainless

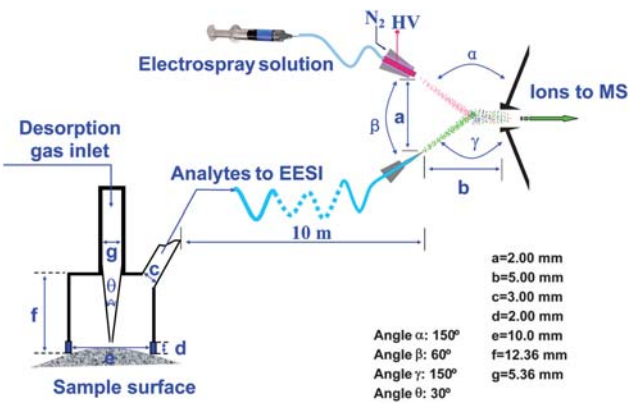

Fig. 1 Schematic diagram of the geometry-independent neutral desorption device coupled to EESI-MS. Note that the diagram is not proportionally scaled.

steel, ID 10 mm; OD 12 mm, length 12.36 mm) to sample surfaces. Thus, the sample collector prevented any analyte liberated by the ND gas from escaping from the collector. Assisted by the nitrogen gas flow inside the sample collector, the analyte plume was guided into the EESI source through a sample transfer line (Teflon tube, ID 3 mm; OD 5 mm, length *ca.* 0.1–10 m) for ionization.

2.3 GIND-EESI-MS analysis

Nitrogen gas, regulated by a valve, was used as the desorption gas. Trace amounts of explosives were immediately sampled using the GIND device when they were deposited onto the substrate surfaces. A homemade EESI source was coupled to a Thermo Finnigan LTQ-XL mass spectrometer (San Jose, CA, USA). Analytes were subjected to ionization in the EESI source. The sample outlet formed an angle of 60° (β) with the electrospray beam, resulting in a distance (a) of 2 mm between the two tips. The angle (α) between the electrospray beam and the heated capillary of the LTQ instrument, and the angle (γ) formed by the sample outlet and the heated capillary of the LTQ instrument were both 150°. The whole EESI assembly was coaxially mounted to the heated capillary of the LTQ instrument, allowing the distance (b) between the inlet of the LTQ instrument and the EESI source to be 5 mm.

A solution of methanol/water/acetic acid (−) or ammonium acetate (+) (50:48:2) was electrosprayed with an infusion rate of 5 μL/min to produce the reagent ions. The LTQ instrument was operated in the positive or negative ion detection mode, depending on the analytes used. The signal intensity is shown in the unit of counts per second (cps). Collision-induced dissociation (CID) experiments were done by applying 18–35% (manufacturer defined energy unit) collision energy to the precursor ions isolated with a mass/charge window of 1 unit. As suggested by the manufacturer, the default values of other parameters such as voltages for the heated capillary, ion optics, and the detectors were directly used without further optimization. All the mass spectra shown here were recorded with an average time of 1 min.

3. Results and discussion

3.1 Characterization of GIND-EESI

Signal of RDX detected using GIND-EESI-MS. In the typical EESI experiment previously reported,[56] liquid samples were sprayed into the electrospray beam, where micro liquid droplet–droplet extraction/ionization occurs, providing an extraction-based process. In our current work, analytes were introduced into the electrospray beam through the sample transfer line. RDX (MW 222) was selected as a test explosive to characterize the ND-EESI source and to optimize the working conditions. Fig. 2 shows the protonated RDX molecules (m/z 223) in the full scan EESI-MS spectrum recorded from RDX (1 ng) on a paper surface. The detection of RDX was confirmed by the fragments observed in the MS/MS spectrum (inset of Fig. 2). The major fragments of m/z 177, 207, and 163 were generated by the loss of NO_2, O, and CH_2NO_2, respectively. The fragmentation pattern was in consistent with those previously observed.[21,22,41,44] These data showed that the homemade ND-EESI source worked for the direct detection of non-volatile compounds on surfaces.

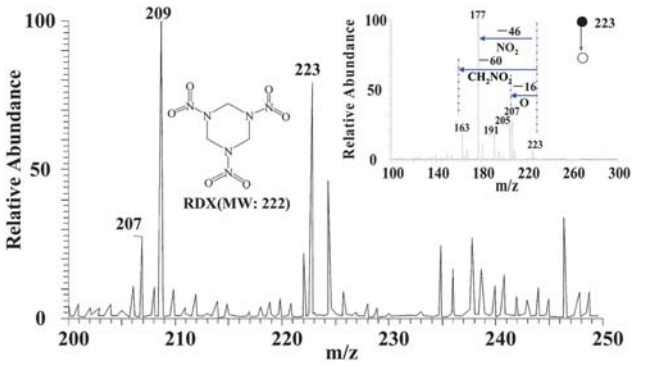

Fig. 2 Typical mass spectra of RDX recorded from a paper surface using GIND-EESI-MS. The inset shows the MS/MS spectrum of the protonated RDX (m/z 223).

Effect of the ND gas flow. It was found that the pressure of the neutral desorption gas played important roles in maintaining a stable signal of RDX (m/z 223). The effect of the gas pressure on the signal levels of RDX was experimentally investigated using the major fragment (m/z 177) detected in the MS/MS experiment. The signal levels increased dramatically until the desorption gas pressure got up to 1.4 MPa, probably because the efficiency for the liberation of RDX from the surface was increased (Fig. 3a). The signal level was almost constant when the gas pressure was between 1.4 and 1.8 MPa, and then decreased quickly when the gas pressure was further increased over 1.8 MPa. No signal of RDX (m/z 177 in MS/MS spectrum) was detected once the gas pressure was higher than 3 MPa, probably because the gas flow rate was too high for the EESI to ionize the analytes. Therefore, the neutral desorption gas pressure was set at 1.6 MPa.

Theoretically, any type of gases can be used as the desorption gas for neutral desorption sampling. It is not surprising that pressured air, nitrogen, argon, and carbon dioxide show no detectable difference for sampling RDX on surfaces, because these gas molecules are of similar size and molecular weight. It is also worth noting that reactive chemical species may have different desorption behaviors when these gases are used, especially in cases where chemical reactions are expected between analytes and major components of the gas beam. Due to its wide availability, nitrogen gas was used as the ND gas for all the following experiments.

Effect of the distance between the sample surface and the gas emitter. It was found that the signal intensities of RDX (m/z 177 in MS/MS spectrum) were heavily dependent on the distance between the gas emitter and the sample surface. Fig. 3b shows the relationship between the distance and the signal levels. Apparently, the shorter the distance is, the higher the signal can be. For all the tested data points, the signal levels (cps) and the desorption distance (cm) were closely fitted using a function $\log(y) = -1.15 \log(x) + 1.68$, showing a fitting coefficient of $R^2 = 0.95$. According to this equation, it is necessary to put the gas emitter infinitely close to the sample surface in order to obtain the most abundant signal. This is applicable for many solid surfaces such as stainless steel, plastics, *etc*. For surfaces containing soft and/or fragile matrices, the distance between the

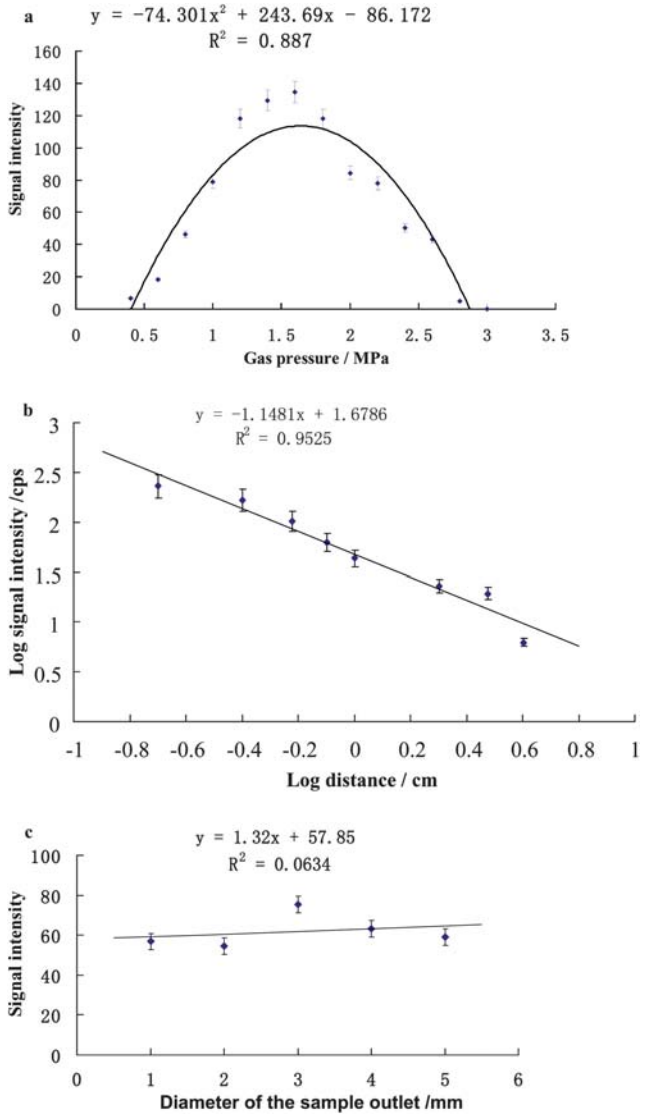

Fig. 3 Optimization of the neutral desorption conditions for surface sampling: (a) effect of the gas pressure on the signal intensity; (b) effect of the distance between the gas emitter and the sample surface on the signal intensity; (c) effect of the inner diameter of the sample outlet on the signal intensity. Note that the signal intensities of *m*/*z* 177 obtained in MS/MS experiments were used for the parameter optimization. Each data point designates the average of 8 measurements. The error bars show the standard deviations of data point.

gas emitter and the sample surface should not be too close to avoid the destructive sampling process caused by the strong gas beam. This is important for biological applications, especially for the *in vivo* characterization of living objects such as green plants, tender human skin, *etc*. Therefore, the distance between the gas emitter and the sample surface was set at 6 mm in this study.

Effect of the volume and material of the GIND device. The sampled analytes might be partially lost during the transportation along the GIND chamber and sample transfer line. No significant sensitivity change was observed for GIND devices with volumes ranging from 1 to 5 cm^3, probably because all the materials desorbed from the sample surface were efficiently transferred to the EESI source without notable loss. However, the signal dropped down to half when a large volume (20 cm^3) was used. It was also found that the signal loss could be reduced using a high gas flow rate for GIND devices of large volumes. This is a very useful feature, making it possible to efficiently transfer the analytes over a long distance. Consequently, remote analysis can be carried out using the GIND device. In addition, the GIND device and the sample transfer line should not be made from materials of high affinities to the analytes. For explosives detection, the inert materials such as stainless steel, glass, and Teflon have shown very similar sensitivity in our experiments.

The volume of the GIND device affects the signal response time. The signal delay time could be more than 6 s once the volume was over 50 cm^3. On the other hand, the same delay could be observed when the sampled analytes were transferred over 20 m. As discussed later, the delay time is seriously dependent on the velocity of the carrier gas inside the sample transfer line.

Effect of the diameter of the sample outlet. As shown in Fig. 3a, the gas pressure at the sample outlet affects the EESI process and thus the signal intensity. Once the gas pressure was set to be 1.6 MPa, the signal abundances were kept at similar levels regardless of the sample outlet diameter (Fig. 3c, R^2 is small). The possible reason could be that the velocity of the gaseous stream could not change significantly when the inner diameter of the sample outlet varied from *ca.* 1–5 mm. Once the gas flux (*i.e.*, the gas pressure) was dramatically changed, the EESI conditions should be greatly altered and thus result in unstable signals.

To be noted, the optimized conditions mentioned above are only related to the neutral desorption process, thus they can be applied to both the positive ion and negative ion detection modes. To make use of ion/molecule reactions for selective explosives detection (see the section below), a solution of methanol/water/acetic acid (50:48:2) was used as the spray solution for the negative ion detection mode, and a solution of methanol/water/ammonium acetate (50:48:2) was used for the positive ion detection mode. The other working conditions of EESI were selected as follows: an infusion rate of 5 μL/min, and a high voltage of 3.5 kV. When the infusion rate was lower than 0.5 μL/min and/or the high voltage was less than 1.5 kV, the signal intensity was much lower. For safety reasons, higher voltages for the ESI were not investigated.

3.2 Explosives detection

Explosives are typical compounds of extremely low vapor pressure. Typical explosives such as TNT, RDX, HMX, TNB, HMTD, TATP, and NG were selected as the representative compounds for experiments. As shown in Fig. 4a, TNT (1 pg) on a paper surface was detected as radical anions (*m*/*z* 227) using GIND-EESI-MS under the negative ion detection mode. In the CID spectrum (inset of Fig. 4a), the radical anion of TNT (*m*/*z* 227) generated fragments of *m*/*z* 212, 210, 197, and 183 by the loss of CH_3, OH, NO, and probably $NOCH_2$, respectively. The TNT fragmentation data were identical to those obtained in previous studies,[22,44] which confirmed that TNT was successfully detected using GIND-EESI-MS.

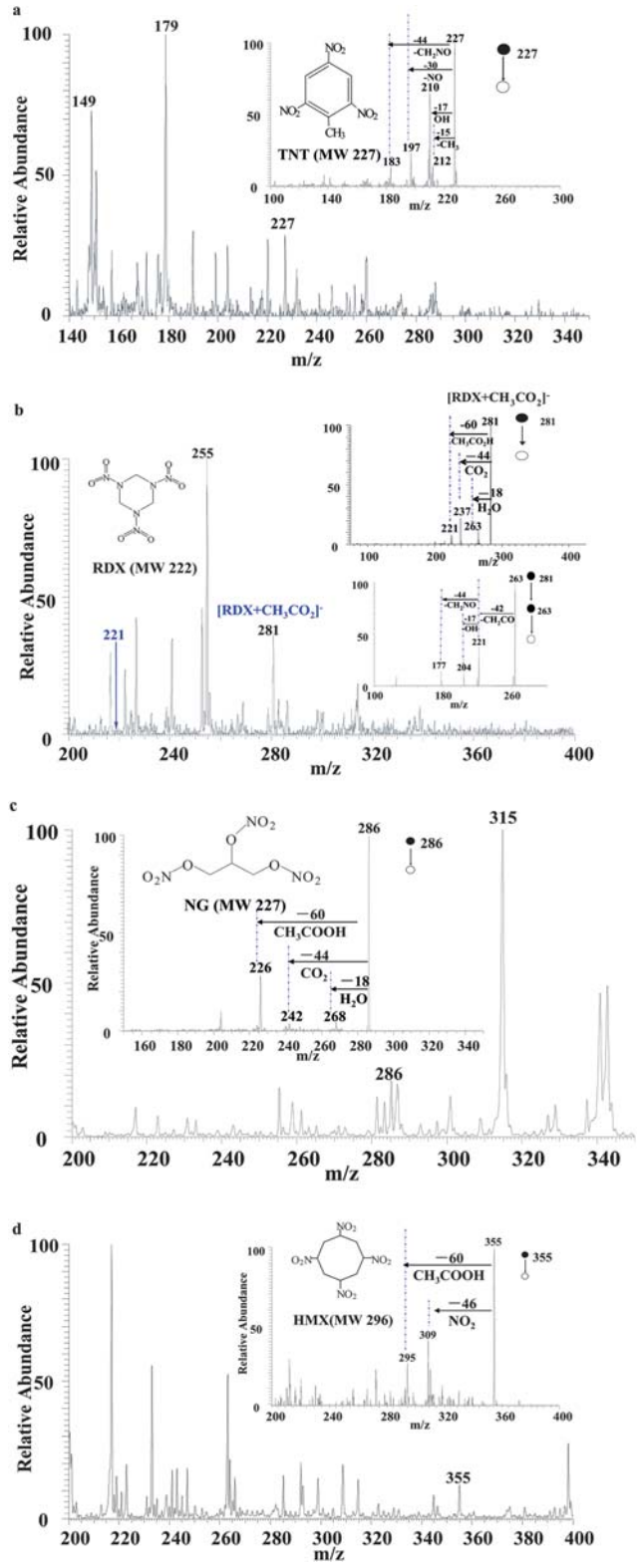

Fig. 4 Detection of explosives using GIND-EESI-MS/MS under the negative ion detection mode: (a) TNT mass spectra, the inset shows the MS/MS spectrum of the radical anion of TNT (*m*/*z* 227); (b) observation of $(RDX + CH_3COO)^-$ complexes (*m*/*z* 281), the inset shows the characteristic fragments of the complexes (*m*/*z* 281); (c) observation of $(NG + CH_3COO)^-$ complexes (*m*/*z* 286), the inset shows the characteristic fragments of the complexes (*m*/*z* 286); (d) observation of $(HMX + CH_3COO)^-$ complexes (*m*/*z* 355), the inset shows the characteristic fragments of the complexes (*m*/*z* 355). Note that all these mass spectra were collected by electrospraying acetic acid in methanol/water solution (2:50:48, v:v:v) using the negative ion detection mode.

Many explosives such as RDX, HMX, and NG can be detected as negative ions by forming ionic clusters with negative ion ligands.[25,61,62] It is highly desirable to improve reliability for the detection of trace levels of explosives present in complex matrices by using tandem mass spectrometry and/or selective ion/molecule reactions. Selective detection of analytes such as sulfur-containing non-polar compounds[63] and diethylene glycol[64] in toothpaste has been demonstrated using reactive EESI-MS. In this study, deprotonated acetic acid $(CH_3COO)^-$ formed by electrospraying the acetic acid in methanol/water solution (2:50:48, v:v:v) was used as the reagent ions to selectively react with explosives such as RDX, NG, and HMX, providing abundant signals at *m*/*z* 281 (Fig. 4b), 286 (Fig. 4c), and 355 (Fig. 4d) by the formation of complexes of $(M + CH_3COO)^-$. Upon CID, the precursor ions of *m*/*z* 281 produced major fragments of *m*/*z* 263, 237 and a small peak at *m*/*z* 221 (inset of Fig. 4b) by the loss of water, CO_2, and acetic acid, respectively. The product ions of *m*/*z* 263 further fragmented to yield ions of *m*/*z* 221, 204 and *m*/*z* 177 in the MS^3 spectrum (inset of Fig. 4b) by the loss of CH_2CO, $C_2H_3O_2$ and $C_3H_4NO_2$, respectively. Our data show that $(RDX + CH_3COO)^-$ was preferably formed rather than deprotonated RDX ions, which were undetectable under the experimental conditions (shown in Fig. 4b). Upon CID (inset of Fig. 4c), ions of *m*/*z* 286 fragmented to form ionic residues at *m*/*z* 268, 242, and 226 by the loss of water, CO_2, and CH_3COOH, respectively. The precursor ions (*m*/*z* 355) formed by HMX and CH_3COO^- ions gave fragments of *m*/*z* 309 and *m*/*z* 295 by the loss of NO_2 and CH_3COOH, respectively, in the MS/MS spectrum (inset of Fig. 4d). Table 1 summarizes the characteristic fragments observed during these experiments. Note that no molecular ions of explosives were predominantly generated in the CID experiments of complexes of $(M + CH_3COO)^-$. These characteristic fragments confirm the successful detection of the explosives. Meanwhile, these data indicate that the $(RDX + CH_3COO)^-$ complex rather than non-covalent bonds was formed, thus the specificity of detection was further improved by using reactive EESI.

Reactive EESI using ammonium acetate aqueous solution (2%) was also applied to detect explosives such as TATP, TNB, and HMTD. Fig. 5a shows the EESI mass spectra of TATP (MW 222, 10 pg), a widely used explosive containing no nitryl group, recorded from human skin using positive ion detection mode. Interestingly, TATP signals showed up at *m*/*z* 223 and *m*/*z* 240, which corresponded to the protonated molecule and proton bound ammonia cluster, respectively. Upon CID, the protonated TATP molecules (*m*/*z* 223) generated fragments of *m*/*z* 208 and *m*/*z* 207 by the loss of CH_3 and O, respectively. As shown in the inset of Fig. 5a, the ions (*m*/*z* 240) produced ionic species of *m*/*z* 225, 223, and 222 by the loss of CH_3, NH_3, and water, respectively. In MS^3, the fragment (*m*/*z* 225) cleaved NH_3 to yield ions of *m*/*z* 208, while the ions of *m*/*z* 222 lost CH_3 to give a major fragment at *m*/*z* 207. Due to the rich amount of sodium on skin surface, the $(TATP + Na)^+$ complexes (*m*/*z* 245) were also

Table 1 Characteristic fragments of explosives observed using reactive EESI-MS/MS

	Observed ions in full scan MS				
Explosives (detection mode)	MW	Ionic species	*m/z*	MS^2 product ions *m/z*	Neutral loss from MS^2
TNT (−)[a]	227	$[M]^-$	227	212, 210, 197, 183	CH_3, OH, NO, $NOCH_2$
RDX (−)[a]	222	$[M + CH_3CO_2]^-$	281	263, 237, 221	H_2O, CO_2, CH_3COOH
TATP (+)[b]	222	$[M + NH_4]^+$	240	225, 223, 222	CH_3, OH, H_2O
HMX (−)[a]	296	$[M + CH_3CO_2]^-$	355	309, 295	NO_2, CH_3COOH
TNB (+)[b]	213	$[M + H_2O + NH_4]^+$	249	231, 185	H_2O, $[H_2O + NO_2]$
HMTD (+)[b]	208	$[M + H_2O + NH_4]^+$	244	227, 226, 209, 179, 161	NH_3, H_2O, $[NH_3 + H_2O]$, $[NH_3 + H_2O + HCOH]$, $[NH_3 + 2H_2O + HCOH]$
NG (−)[a]	227	$[M + CH_3CO_2]^-$	286	268, 242, 226	H_2O, CO_2, CH_3COOH

[a] The electrospray solvent was a methanol:water:acetate acid mixture (50:48: 2, v/v/v). [b] The electrospray solvent was a methanol:water:ammonium acetate mixture (50:48: 2, v/v/v).

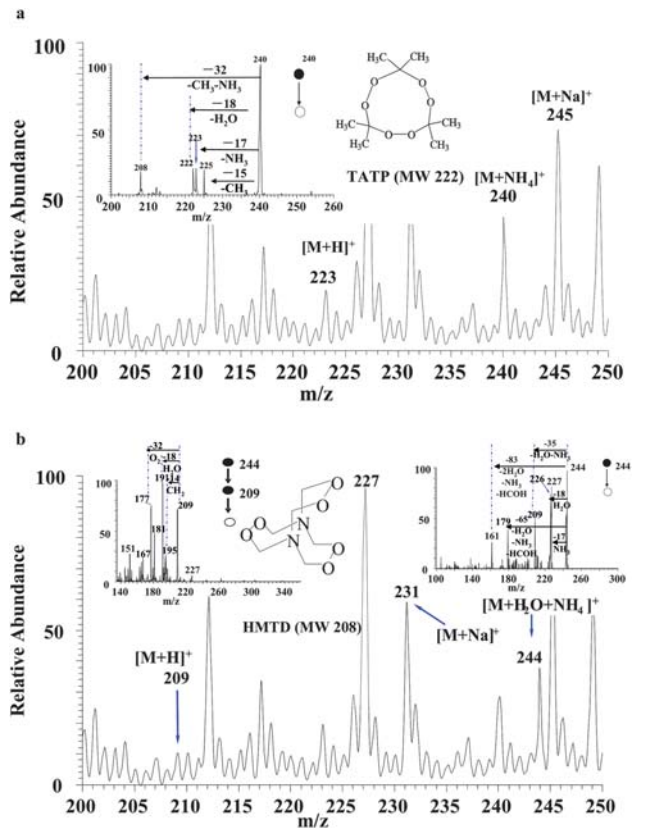

Fig. 5 Detection of TATP and HMTD on human skin surfaces using GIND-EESI-MS. (a) TATP signals at *m/z* 223, 240, and 245 by forming the $(M + H)^+$, $(M + NH_4)^+$, and $(M + Na)^+$ ions. The inset shows the MS/MS spectrum of the complexes (*m/z* 240); (b) HMTD signals detected at *m/z* 209, 231, and 244 by forming the $(M + H)^+$, $(M + Na)^+$ and $(M + H_2O + NH_4)^+$ ions. The insets show the CID mass spectra of $(M + H_2O + NH_4)^+$ ions.

detected with an abundant signal in the EESI-MS spectrum (Fig. 5a). The sodium ions were retained in the residue of the complex (*m/z* 245) under the CID conditions, giving a major product ion at *m/z* 215 by the loss of ethane.[61] The $(TATP + Na)^+$ complex was formed in the EESI step, and neutral TATP molecules or neutral complexes (*i.e.*, TATP + Na-counterion) could also be directly sampled from the skin. The observation of both sodium adducts and protonated TATP shows the gentle character of the GIND-EESI method for the ionization of this extremely fragile molecule.[61] Fig. 5b shows the mass spectra of HMTD obtained using reactive GIND-EESI-MS. The signals detected at *m/z* 209, 231, and 244 were corresponding to the protonated HMTD, sodiated HMTD, and the ionic cluster of $(HMTD + H_2O + NH_4)^+$, respectively. As shown in the insets of Fig. 5b, the precursor ions (*m/z* 244) generated major fragments of *m/z* 227, 226, 209, 179, and 161 by the loss of NH_3, H_2O, $[NH_3 + H_2O]$, $[NH_3 + H_2O + HCOH]$, and $[NH_3 + 2H_2O + HCOH]$, respectively. In the MS^3 spectrum, the fragment ions of *m/z* 209 yielded fragments of *m/z* 195, 191, and 177 by the loss of CH_2, H_2O, and O_2, respectively. These fragmentation patterns were identical as those of the precursor ions of *m/z* 209, which showed up as a small peak (*m/z* 209) in the full scan MS spectrum. The sodiated HMTD ions retained sodium during the CID experiments, producing major fragments of *m/z* 217, 203, and 199 by the loss of CH_2, $[CH_2, CH_2]$, and O_2, respectively. Thus, these data confirmed the successful detection of HMTD using GIND-EESI-MS/MS. Similarly, other explosive compounds could also be detected using this method. Table 1 summarizes the characteristic fragments observed using tandem reactive EESI-MS. Note that explosives such as TNB, HMX, and TATP are difficult to be protonated/deprotonated to give signals for the sensitive detection. Our data suggest that reactive GIND-EESI-MS is attractive for enhancing the sensitivity and specificity of explosive detection.

To explore the sampling mechanism, experiments were also done on a stainless steel surface at different temperatures. To obtain different surface temperatures, the stainless steel surface was heated using water bath at 31 °C, 35 °C, 40 °C, and 45 °C, respectively, for 30 min allowing the thermal equilibrium between the metal and water. A certain amount of RDX (10 ng in 10 μL methanol solution) was deposited on the metal surface to form a sample spot area less than 1 cm^2. The sample spot was placed under the GIND sampling probe by following the procedure described in the Experimental section while the neutral desorption gas (room temperature, 25 °C) was turned on or off. In addition, the neutral desorption gas could be heated up to *ca.* 50–60 °C by heating the gas transfer line (copper tube, ID 1.6 mm; OD 2 mm) up to about 200 °C. Table 2 summarizes the experimental data. The data show that the temperature of the

Table 2 Summary of the signal responses to different temperatures of the surface and the neutral desorption gas

Experiment code	Neutral desorption gas		Metal surface temperature[a] (°C)	Amount of RDX (ng)	Signal level[b]
	ON/OFF	Temperature (°C)			
1	OFF	25	31	1.0	N/A[c]
2	OFF	25	35	1.0	N/A
3	OFF	25	40	1.0	N/A
4	OFF	25	45	1.0	N/A
5	OFF	25	45	10	N/A
6	OFF	25	45	100	N/A
7	ON	25	31	1.0	2.5×10^3
8	ON	25	35	1.0	2.4×10^3
9	ON	25	40	1.0	2.6×10^3
10	ON	25	45	1.0	2.1×10^3
11	ON	50	31	1.0	2.0×10^3
12	ON	50	35	1.0	2.3×10^3
13	ON	60	40	1.0	2.5×10^3
14	ON	60	45	1.0	2.4×10^3
15	OFF	60	45	100	N/A

[a] The variation of temperature was less than ±1 °C. [b] The signal was measured using the characteristic fragment (*m/z* 237) generated in the MS^2 experiments. [c] N/A means that the signal was not detectable (under the noise level) during the experiments.

metal surface and/or the ND gas beam imposes no much effect upon the signal levels of the explosives. Therefore, it is suggested that the explosives were sampled based on a desorption mechanism. These findings also suggest that GIND works only as a sampling probe, which might be coupled to any other detection technique to facilitate the sensitive analysis on surfaces with improved convenience.

The reliability of explosives detection. The explosives could also be detected from various surfaces such as gloves, paper, leather, plastic, and human skin, showing a good reliability of explosives detection using GIND-EESI-MS. For example, Fig. 6a shows a typical ion chromatogram trace of *m/z* 249 corresponding to the existence of TNB on various surfaces. The signal responded quickly to the TNB compound on the surfaces. The signal level reached its 90% maximal height within 2 scans when the explosives such as TNB were exposed to the GIND sampling probe, and the signal decreased down to the background levels within 2 scans once the explosive samples were removed from the GIND sampler. Similar results were obtained for all the explosives tested on various surfaces using the characteristic signals obtained either in full scan mass spectra or CID mass spectra. Note that blank experiments were done properly for all the explosives. No explosive was detected from the blank experiments, and the signal was consistent with the background of the ion chromatogram traces obtained in the explosives detection experiments.

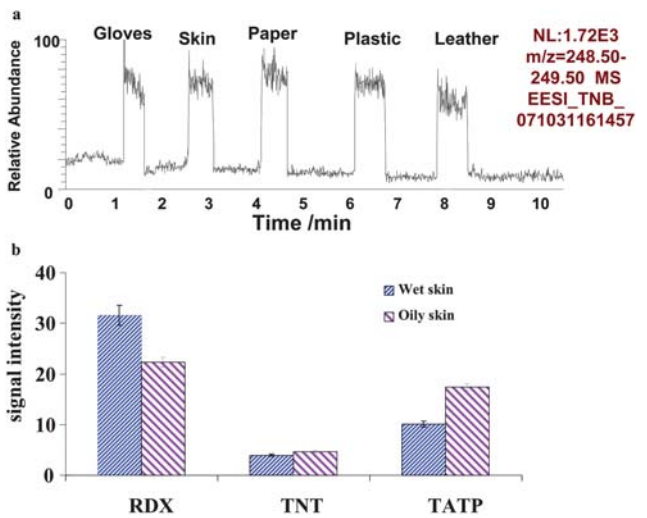

Fig. 6 Signal responses observed from various surfaces: (a) typical ion chromatogram traces of *m/z* 249 corresponding to TNB on various surfaces; (b) signal levels of the characteristic fragments derived from the same amounts of TNT, RDX and TATP on different skin surfaces. Each data point designates the mean value of 8 measurements.

Effect of the surface wetness on the signal intensities of RDX, TNT, and TATP. Extra experiments were performed to examine the effect of surface wetness on the signal levels of explosives. Fig. 6b shows the signal intensities of RDX, TNT, and TATP on a water/sweat-wetted human skin surface and on an oily human skin surface. It is clearly shown that the signal levels are related to the substrate surfaces. This is probably because explosives have distinct affinities for different surfaces. These findings indicate that the quantitative detection of explosives on different surfaces requires calibration curves made on the specific surfaces.

The inert rubber installed on the bottom of the geometry-independent neutral desorption device makes the GIND device fit tightly on any solid surface when it is pressed. The small air-tight enclosure with fixed space between the GIND gas emitter, sample surface, and sample collector requires no optimization of the GIND device when it is applied to solid sample surfaces. This greatly facilitates the high-throughput analysis of untreated samples. The spatially fixed GIND device also improves the reproducibility of measurements leading to enhanced precision for the trace detection of explosives.

3.3 Sensitivity and dynamic response range

Using the GIND device reported here, all the materials sampled from the surfaces can be transferred to the EESI source without noticeable material loss. Thus, the sensitivity for explosives detection can be significantly improved. Low LOD (limit of detection) values ranged between 59 and 842 fg ($S/N \geq 3$) were obtained using the major fragments of explosives in the GIND-EESI-MS/MS experiments. Table 3 summarizes the LOD data for all the explosives tested using various surfaces. Fig. 7 shows the selected ion current for the signals of $[TATP + NH_4]^+$ complexes (upper panel) and protonated TATP (lower panel). Note that these signals were validated by using MS/MS data as described in the above sections. It is evident that the sensitivity of this method relies on the molecular interaction between the explosives and surfaces. As shown in Table 3, the signal levels of the explosives were clearly surface-related.

Acceptable relative standard deviation (RSD) values were obtained using GIND-EESI-MS for all the explosives tested on various surfaces. Typical RSD values for explosives (1 pg) on paper, gloves, metal, leather, *etc.*, were in the range of *ca.* 4.6–10.2%, showing reasonable reproducibility for measuring

Table 3 LOD values (total amount, fg) of explosives detected on various surfaces using GIND-EESI-MS/MS[a]

Explosives	Ionic precursors	Signal[b] (*m*/*z*)	Skin	Gloves	Textiles	Plastics	Paper	Leather	Glass
TNT (−)	$[M]^-$	197	216	250	273	618	222	370	682
RDX (−)	$[M + CH_3CO_2]^-$	237	533	103	574	203	726	432	107
TATP (+)	$[M + NH_4]^+$	225	297	365	240	390	275	183	268
HMX (−)	$[M + CH_3CO_2]^-$	309	764	429	736	136	798	343	728
TNB (+)	$[M + H_2O + NH_4]^+$	231	110	350	340	361	600	730	780
HMTD (+)	$[M + H_2O + NH_4]^+$	227	253	400	330	328	560	526	704
NG (−)	$[M + CH_3CO_2]^-$	268	170	59	808	106	127	842	701

[a] The RSD values ranged from 4.6% to 10.2% for 8 measurements on the same sample. [b] Signals were the characteristic fragments observed in the MS/MS spectra.

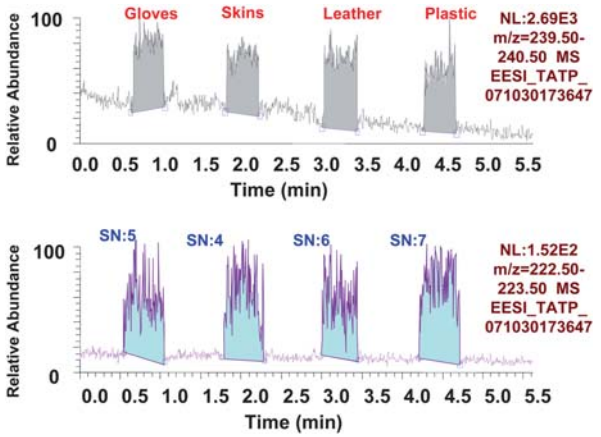

Fig. 7 Signals correlated to trace levels of TATP detected from various surfaces using GIND-EESI-MS. The upper panel shows the ion chromatogram corresponding to the ionic complexes (*m*/*z* 240); the lower panel shows the total ion current trace of the protonated TATP molecules (*m*/*z* 223).

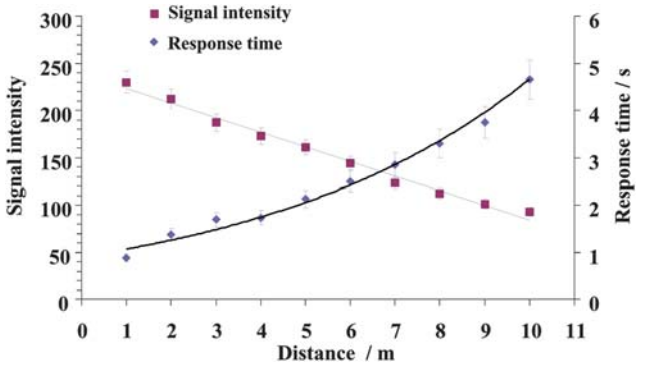

Fig. 8 Signal responses and time delay observed in remote explosives detection using GIND-EESI-MS. A linear relationship between the sample transportation distance (x) and the signal intensity (y) was fitted by the equation $y = -12.109x + 209.4$, $R^2 = 0.990$; the time delay (t) of the signal as a function of the sample transportation distance (x) was described by the equation $t = 0.9055e^{0.1639x}$, $R^2 = 0.969$.

trace levels of explosives on untreated surfaces. For a given surface such as a paper surface, linear responses for all the explosives tested were in the range of picograms to nanograms (data not shown). Thus, this method is suitable for fast screening the presence of explosives, and is also very promising for the quantitative analysis of explosives on surfaces of different materials.

3.4 Remote explosives analysis and safety

A significant advantage of using the sealed GIND device is that analytes sampled from surfaces can be transferred over a long distance with no serious sensitivity loss. For the detection of explosives in the real world, remote analysis is preferable, especially under hazardous or risky environments. The concept of remote explosives detection was demonstrated by Cotte-Rodriguez and Cooks using DESI.[62] Explosives (total amounts of 0.5–20 ng) were sampled over a distance of *ca.* 1–3 m in the ambient conditions for the remote mass detection.[62] In the present study, the characteristic fragments of (RDX + $CH_3COO)^-$ were detected in GIND-EESI-MS/MS by transferring neutral RDX molecules sampled from hand surfaces along a Teflon tube (10 m length; 3 mm ID) to the EESI source. The signal intensity of the RDX fragment (*m*/*z* 237) maintained an almost constant value for different lengths of the sample transfer line. However, signal responses were delayed for a few seconds once the sample transfer line was longer than 3 m. Fig. 8 shows the signal levels and the response delay detected by transferring the neutral explosive molecules over different distances. The signal delay time (t) fits into an equation of $t = 0.9055e^{0.1639x}$, $R^2 = 0.969$, showing that a delay time of about 24 s is expected when the distance (x) is over 20 m. Fortunately, the signal delay can be reduced by accelerating the velocity of the carrier gas (*e.g.*, using a high gas flow rate and/or a narrow sample transferring line with reduced diameter). In the current setup, it takes only milliseconds to obtain an EESI-MS spectrum using the LTQ instrument. Once the sample transfer speed is increased, the signal abundance should be increased accordingly. Furthermore, the geometry-independent ND device required no optimization when the sample was reloaded for the GIND-EESI process, which further facilitates the fast analysis of explosives in complex matrices. Our experimental data showed that no serious sample carryover effect was found when a Teflon tube (10 m length; 3 mm ID) was used. Therefore, an overall acceptable analysis speed has been achieved by using this method for fast screening the presence of trace amounts of explosives on various surfaces.

Due to the ability of remote analysis, the GIND device provides a safe detection method which can be used directly in many practical applications. For example, in a typical *in vivo*

analysis, traditional ambient methods require the use of organic solvents and high voltages on/near biological surfaces, which might be harmful to living objects and cause high risks to them. In contrast, a desorption gas such as nitrogen is used to flow over surfaces in GIND-EESI-MS experiments, keeping the objects under evaluation away from any chemical contamination or charged particle bombardment. In addition, the GIND-EESI setup is highly recommended for detection under extreme environments, because instrument operators can stay as far as 20 m away from the sampling location.

4. Conclusions

Neutral desorption sampling on virtually all types of surfaces is made easier and more robust by using the GIND device. The GIND device has the advantages of easy fabrication, convenient use, efficient neutral sample transfer, and high sensitivity without significant material loss after the ND process. The operating parameters of the new ND device, including desorption gas composition, surface wetness, gas flow rate, internal diameter of the sample outlet, and device material, were experimentally investigated. Data obtained under the optimized experimental conditions have shown that GIND is capable of sampling explosives at sub-picogram levels directly from various surfaces including human skin, gloves, envelopes, plastic, clothes, *etc.*, for the rapid and sensitive detection by EESI-MS^n. The limit of detection for most explosives was *ca.* 59–842 fg/cm^2 ($S/N = 3$, $n = 8$) on the untreated surfaces of different materials. Typical RSD values for trace amounts of explosives measurements were in the range of *ca.* 4.6–10.2%, providing reasonable reproducibility. No optimization of the GIND device and the EESI source conditions was required when samples were reloaded, facilitating the fast screening of explosives on untreated surfaces. A single sample analysis could be completed within a few seconds by using a short sample transfer line (less than 20 cm). In addition, successful transportation of neutral analytes over a distance longer than 10 m was demonstrated without either significant signal loss or long signal response delay (more than 10 s), showing that ND-EESI-MS is a promising way for fast, sensitive, and remote explosives detection.

Acknowledgements

This work was jointly supported by the MOST of China (Innovation Method Fund, No. 2008IM040400, SSSTC grant, No. 2009DFA30800) and another grant from HIT (IMJQ10070004).

References

1 X. P. Pan, M. J. San Francisco, C. Lee, K. M. Ochoa, X. Z. Xu, J. Liu, B. H. Zhang, S. B. Cox and G. P. Cobb, *Mutat. Res., Genet. Toxicol. Environ. Mutagen.*, 2007, **629**, 64–69.
2 H. N. Banerjee, M. Verma, L. H. Hou, M. Ashraf and S. K. Dutta, *Yale J. Biol. Med.*, 1999, **72**, 1–4.
3 J. I. Steinfeld and J. Wormhoudt, *Annu. Rev. Phys. Chem.*, 1998, **49**, 203–232.
4 P. Le Barny, E. Obert, V. Simic and I. Leray, *Actual. Chimique*, 2007, 104–107.
5 A. N. Martin, G. R. Farquar, E. E. Gard, M. Frank and D. P. Fergenson, *Anal. Chem.*, 2007, **79**, 1918–1925.
6 L. Nyadong, M. D. Green, V. R. De Jesus, P. N. Newton and F. M. Fernandez, *Anal. Chem.*, 2007, **79**, 2150–2157.
7 A. Venter, D. R. Ifa, R. G. Cooks, S. K. Poehlein, A. Chin and D. Ellison, *Propellants, Explos., Pyrotech.*, 2006, **31**, 472–476.
8 J. R. Verkouteren, *J. Forensic Sci.*, 2007, **52**, 335–340.
9 B. M. Kolakowski and Z. Mester, *Analyst*, 2007, **132**, 842–864.
10 R. Schulte-Ladbeck, A. Edelmann, G. Quintas, B. Lendl and U. Karst, *Anal. Chem.*, 2006, **78**, 8150–8155.
11 N. R. Walker, M. J. Linman, M. M. Timmers, S. L. Dean, C. M. Burkett, J. A. Lloyd, J. D. Keelor, B. M. Baughman and P. L. Edmiston, *Anal. Chim. Acta*, 2007, **593**, 82–91.
12 B. Johnson-White, M. Zeinali, K. M. Shaffer, C. H. Patterson, P. T. Charles and M. A. Markowitz, *Biosens. Bioelectron.*, 2007, **22**, 1154–1162.
13 R. L. Marple and W. R. LaCourse, *Anal. Chem.*, 2005, **77**, 6709–6714.
14 R. L. Marple and W. R. LaCourse, *Talanta*, 2005, **66**, 581–590.
15 J. Wang, S. Thongngamdee and D. L. Lu, *Electroanalysis*, 2006, **18**, 971–975.
16 M. Nagai, *J. Electrochem. Soc.*, 2007, **154**, J65–J70.
17 Gaurav, V. Kaur, A. Kumar, A. K. Malik and P. K. Rai, *J. Hazard. Mater.*, 2007, **147**, 691–697.
18 D. Gaurav, A. K. Malik and P. K. Rai, *Crit. Rev. Anal. Chem.*, 2007, **37**, 227–268.
19 C. R. Bommarito, A. B. Sturdevant and D. W. Szymanski, *J. Forensic Sci.*, 2007, **52**, 24–30.
20 B. V. Pond, C. Mullen, I. Suarez, J. Kessler, K. Briggs, S. E. Young, M. J. Coggiola, D. R. Crosley and H. Oser, *Appl. Phys. B: Lasers Opt.*, 2007, **86**, 735–742.
21 N. Na, C. Zhang, M. X. Zhao, S. C. Zhang, C. D. Yang, X. Fang and X. R. Zhang, *J. Mass Spectrom.*, 2007, **42**, 1079–1085.
22 D. R. Justes, N. Talaty, I. Cotte-Rodriguez and R. G. Cooks, *Chem. Commun.*, 2007, 2142–2144.
23 J. A. Mathis and B. R. McCord, *Rapid Commun. Mass Spectrom.*, 2005, **19**, 99–104.
24 Z. Takats, I. Cotte-Rodriguez, N. Talaty, H. W. Chen and R. G. Cooks, *Chem. Commun.*, 2005, 1950–1952.
25 A. Venter and R. G. Cooks, *Anal. Chem.*, 2007, **79**, 6398–6403.
26 C. Mullen, A. Irwin, B. V. Pond, D. L. Huestis, M. J. Coggiola and H. Oser, *Anal. Chem.*, 2006, **78**, 3807–3814.
27 C. A. Groom, A. Halasz, L. Paquet, S. Thiboutot, G. Ampleman and J. Hawari, *J. Chromatogr., A*, 2005, **1072**, 73–82.
28 J. K. Lokhnauth and N. H. Snow, *J. Chromatogr., A*, 2006, **1105**, 33–38.
29 A. C. Schmidt, B. Niehus, F. M. Matysik and W. Engewald, *Chromatographia*, 2006, **63**, 1–11.
30 H. W. Chen, H. Z. Liang, J. H. Ding, J. H. Lai, Y. F. Huan and X. L. Qiao, *J. Agric. Food Chem.*, 2007, **55**, 10093–10100.
31 W. T. Ma, W. Chan, K. Steinbach and Z. W. Cai, *Anal. Bioanal. Chem.*, 2007, **387**, 2219–2225.
32 H. W. Chen, N. N. Talaty, Z. Takats and R. G. Cooks, *Anal. Chem.*, 2005, **77**, 6915–6927.
33 Z. Takats, J. M. Wiseman, B. Gologan and R. G. Cooks, *Science*, 2004, **306**, 471–473.
34 R. B. Cody, *Anal. Chem.*, 2009, **81**, 1101–1107.
35 K. Kpegba, T. Spadaro, R. B. Cody, N. Nesnas and J. A. Olson, *Anal. Chem.*, 2007, **79**, 5479–5483.
36 H. W. Chen, J. H. Lai, Y. F. Zhou, Y. F. Huan, J. Q. Li, X. Zhang, Z. C. Wang and M. B. Luo, *Chin. J. Anal. Chem.*, 2007, **35**, 1233–1240.
37 S. P. Yang, J. H. Ding, J. Zheng, B. Hu, J. Q. Li, H. W. Chen, Z. Q. Zhou and X. L. Qiao, *Anal. Chem.*, 2009, **81**, 2426–2436.
38 S. P. Yang, H. W. Chen, Y. L. Yang, B. Hu, X. Zhang, Y. F. Zhou, L. L. Zhang and H. W. Gu, *Chin. J. Anal. Chem.*, 2009, **37**, 315–318.
39 S. P. Yang, B. Hu, J. Q. Li, J. Han, X. Zhang, H. W. Chen, Q. Liu, Q. J. Liu and J. Zheng, *Chin. J. Anal. Chem.*, 2009, **37**, 691–694.
40 K. Chingin, G. Gamez, H. W. Chen, L. Zhu and R. Zenobi, *Rapid Commun. Mass Spectrom.*, 2008, **22**, 2009–2014.
41 H. W. Chen, B. Hu, Y. Hu, Y. F. Huan, Z. Q. Zhou and X. F. Qiao, *J. Am. Soc. Mass Spectrom.*, 2009, **20**, 719–722.
42 L. Zhu, G. Gamez, H. W. Chen, K. Chingin and R. Zenobi, *Chem. Commun.*, 2009, 559–561.
43 J. D. Harper, N. A. Charipar, C. C. Mulligan, X. R. Zhang, R. G. Cooks and Z. Ouyang, *Anal. Chem.*, 2008, **80**, 9097–9104.
44 Y. Zhang, X. X. Ma, S. C. Zhang, C. D. Yang, Z. Ouyang and X. R. Zhang, *Analyst*, 2009, **134**, 176–181.
45 C. Y. Cheng, C. H. Yuan, S. C. Cheng, M. Z. Huang, H. C. Chang, T. L. Cheng, C. S. Yeh and J. Shiea, *Anal. Chem.*, 2008, **80**, 7699–7705.

46 I. X. Peng, R. R. O. Loo, J. Shiea and J. A. Loo, *Anal. Chem.*, 2008, **80**, 6995–7003.
47 J. Shiea, C. H. Yuan, M. Z. Huang, S. C. Cheng, Y. L. Ma, W. L. Tseng, H. C. Chang and W. C. Hung, *Anal. Chem.*, 2008, **80**, 4845–4852.
48 R. Haddad, H. M. S. Milagre, R. R. Catharino and M. N. Eberlin, *Anal. Chem.*, 2008, **80**, 2744–2750.
49 R. Haddad, R. Sparrapan, T. Kotiaho and M. N. Eberlin, *Anal. Chem.*, 2008, **80**, 898–903.
50 R. Haddad, R. R. Catharino, L. A. Marques and M. N. Eberlin, *Rapid Commun. Mass Spectrom.*, 2008, **22**, 3662–3666.
51 J. P. Williams, V. J. Patel, R. Holland and J. H. Scrivens, *Rapid Commun. Mass Spectrom.*, 2006, **20**, 1447–1456.
52 G. M. Huang, H. Chen, X. R. Zhang, R. G. Cooks and Z. Ouyang, *Anal. Chem.*, 2007, **79**, 8327–8332.
53 T. J. Kauppila, N. Talaty, T. Kuuranne, T. Kotiaho, R. Kostiainen and R. G. Cooks, *Analyst*, 2007, **132**, 868–875.
54 Z. Z. Pan, H. W. Gu, N. Talaty, H. W. Chen, N. Shanaiah, B. E. Hainline, R. G. Cooks and D. Raftery, *Anal. Bioanal. Chem.*, 2007, **387**, 539–549.
55 S. Crotti and P. Traldi, *Combin. Chem. High Throughput Screen.*, 2009, **12**, 125–136.
56 H. W. Chen, A. Venter and R. G. Cooks, *Chem. Commun.*, 2006, 2042–2044.
57 H. W. Chen, S. P. Yang, A. Wortmann and R. Zenobi, *Angew. Chem., Int. Ed.*, 2007, **46**, 7591–7594.
58 H. W. Chen and R. Zenobi, *Nat. Protoc.*, 2008, **3**, 1467–1475.
59 H. W. Chen, Y. P. Sun, A. Wortmann, H. W. Gu and R. Zenobi, *Anal. Chem.*, 2007, **79**, 1447–1455.
60 H. W. Chen, A. Wortmann and R. Zenobi, *J. Mass Spectrom.*, 2007, **42**, 1123–1135.
61 I. Cotte-Rodriguez, H. Chen and R. G. Cooks, *Chem. Commun.*, 2006, 953–955.
62 I. Cotte-Rodriguez and R. G. Cooks, *Chem. Commun.*, 2006, 2968–2970.
63 H. W. Chen, A. Wortmann, W. H. Zhang and R. Zenobi, *Angew. Chem., Int. Ed.*, 2007, **46**, 580–583.
64 J. H. Ding, S. P. Yang, Q. Liu, Z. Z. Wu, H. W. Chen, Y. L. Ren, J. Zheng and Q. J. Liu, *Chem. J. Chin. Univ.*, 2009, **30**, 1533–1537.

